

Interface energy and electron structure for Fe/VN

J. Hartford

Department of Applied Physics, Chalmers University of Technology and Göteborg University, SE-412 96 Göteborg, Sweden

(Received 1 February 1999)

The electronic and atomic structures in a model system of the semicoherent interface between bcc-Fe and nacl-VN is studied. Knowledge of interface structure and energetics is important for modeling of nucleation and growth in complex alloys on a thermodynamical level. Present model system is of interest, as such interfaces are common in alloyed steels. For the total energy calculation a pseudopotential (PP) implementation of density-functional theory (DFT) is used. In particular, the code includes ultrasoft PP and the so-called generalized-gradient approximation (PW91) for the DFT exchange and correlation energy. We have calculated interface energies for supercells with a varying VN unit thickness and, in addition to the ideal interface, also interfaces with N vacancies are considered. The Fe/VN interface energy is found to be very small, although the presence of vacancies raises the energy. Experimentally observed VN precipitates are very thin and the calculations point out features of the electron structure that make this smallness favorable.

I. INTRODUCTION

Materials properties ultimately depend on the atoms that constitute the material. For many phenomena this dependence has a hierarchical structure that bridges from atomic up to macroscopic scales.^{1,2} At the mesoscale, interfaces are key features for mechanical and electronical properties.³ In particular, the strength of metals is determined by extrinsic obstacles, such as solute atoms, precipitates, and grain boundaries, which hinder or block the motion of dislocations. To control the appearance and texture of those structures are of prime importance for obtaining the desired properties of a material. Hence, knowledge of interface structure and energetics is important for modeling of complex alloys on a thermodynamical level.

In steels, nonshearable precipitates are obtained with carbide and nitride formers, such as Ti, V, Cr, and Nb.^{4,5} Precipitates with the nacl structure is one important class and are often found as small thin discs (diameter ≈ 100 – 200 Å). The “flat” part of the interface is semicoherent (that is, has a small misfit-dislocation density), whereas the “side” of the disc has a large lattice mismatch and is incoherent with the Fe matrix.^{6,7} These small precipitates form within grains, contrary to other carbides and nitrides, which preferably form on grain boundaries. Modeling of nucleation and growth of such precipitates provide a basis to predict long-time structural changes in a steel. This is of general interest and especially significant for improving high-temperature creep resistance.^{8,9}

In this paper the electronic and atomic structures of a model system for the semi-coherent interface between Fe and VN is studied. Only interfaces for ferritic steels (bcc-Fe) are addressed and such precipitates have their semicoherent interface oriented according to the so-called Baker-Nutting relation,

$$\begin{aligned} \{100\}_{\text{nacl}} // \{100\}_{\text{bcc}} \\ \langle 100 \rangle_{\text{nacl}} // \langle 110 \rangle_{\text{bcc}}. \end{aligned} \quad (1)$$

The interface is simulated by a periodic supercell with some n_{Fe} layers of bcc-Fe. The intermediate nacl-VN layers are oriented according to Eq. (1). Presently, only the chemical contribution to the Fe/VN interface energy is searched for. At $T=0$ K this energy is the difference between the total energy of the combined system and the total energies of the separated bulk parts,

$$\gamma = (E_{\text{Fe/VN}}[n_{\text{Fe}}, n_{\text{VN}}] - E_{\text{Fe}}[n_{\text{Fe}}] - E_{\text{VN}}[n_{\text{VN}}]) / A, \quad (2)$$

where A is the interface area. Results are presented for a varying number (n_{VN}) of VN layers.

The real excess energy of the interface depends on the chemical potentials for each constituent of a particular steel.³ However, for the thermodynamical modeling free-energy data for the bulk are taken from semiempirical Thermo-Calc calculations.^{8,10} In this approach the interface energy defined in Eq. (2) is treated separately. The elastic energies due to volume differences between the two phases may also be included separately within a continuum treatment. Disregarding the creation of misfit dislocations, which would lower the total interface energy, the only unknown quantity is the interface energy in Eq. (2). This energy is prohibitively difficult to establish experimentally and the major purpose of the present paper is to provide good estimates of such interface energies.

The total energy calculation uses a pseudopotential (PP) implementation of density-functional theory (DFT).^{11–13} In this theory the complex many-electron problem is replaced by a simpler approximate one. The approximation of the many-electron exchange and correlation (XC) effects allows for a solution, where a functional of only the electron density is minimized. Methodological advancement of DFT together with the increasing performance of computers and numerical methods have made it realistic to assess the present types of questions from first principles. Here, in particular, ultrasoft pseudopotentials¹⁴ (USPP) are employed, and the XC energy is described in the so-called generalized-gradient approxima-

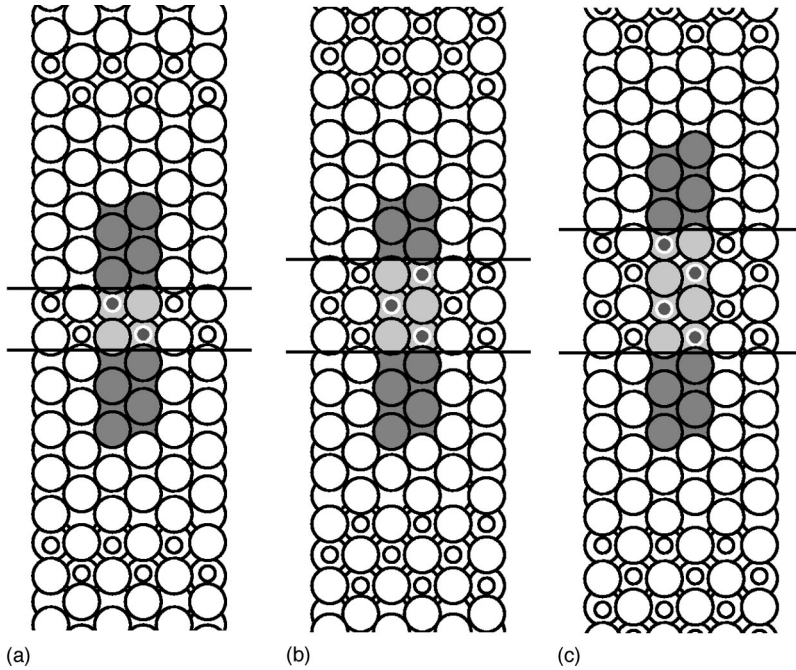


FIG. 1. Selected supercell structures for Fe/VN. Shaded atoms represent the supercell and the rest of the atoms is the periodic repetition. The number of VN layers (n_{VN}) is 2, 3, and 4. The shown supercells have two Fe atoms in each layer above and below the VN unit, which contain 4 atoms in each layer. The side of these supercells are 4.07 Å. The bcc-Fe and nacl-VN structures are oriented according to the Baker-Nutting relation, $\{100\}_{\text{VN}}//\{100\}_{\text{Fe}}$ and $\langle 100 \rangle_{\text{VN}}//\langle 110 \rangle_{\text{Fe}}$.

tion (GGA-PW91).¹⁵ The use of GGA-PW91 is crucial in order to obtain the correct ferromagnetic ground state for Fe.^{16,17}

There are many studies on grain boundaries and semiconductor interfaces in the literature.³ In contrast, few studies on the energetics for heterophase metal-metal interfaces are reported. A system of similar complexity as the present one is the adhesion of NiAl/Cr found in Ref. 18. Other related theoretical work is recent DFT calculations on grain-boundary impurities in Fe and Ni₃Al presented in Refs. 19 and 20, respectively. VN is related to other nitrides and carbides which usually are considered as ceramics. Metal/ceramics interfaces have been studied extensively and a review of theoretical approaches may be found in Ref. 21.

In the next section we describe some details of the DFT calculations and present some bulk system results for Fe, V, and VN and convergence tests. The Fe/VN interface results are then given in Sec. III. The results are discussed in Sec. IV, where also conclusions are drawn. In Sec. V there is a summary.

II. DETAILS OF CALCULATIONS

Total energy calculations within DFT, using a pseudopotential (PP) approximation to replace the core electrons and a plane-wave (PW) basis for the valence electrons, has become a standard model for solids. The introduction of ultra-soft pseudopotentials (USPP) by Vanderbilt has extended its practical use to also include first-row elements.¹⁴ Furthermore, PP have recently been applied successfully to magnetic transition metals, as well.^{22,23} To succeed, a proper treatment of the nonlinear core XC energy is essential, which can be obtained with the partial core correction.²⁴

The length of each interface supercell perpendicular to the layers (z) is $a_z = (n_{\text{Fe}}a_{\text{Fe}}/2 + n_{\text{VN}}a_{\text{VN}}/2)$, where a_{Fe} and a_{VN} are the theoretical equilibrium lattice constants for bulk Fe and VN, respectively. There is a small lattice mismatch ($\approx 1\%$) for the interface (xy) plane. Instead of only expand-

ing Fe or compressing VN, both are slightly strained in the calculation. The stretch of Fe and contraction of VN in a_{xy} are chosen to give equal energy increases per volume for Fe and VN, respectively. This is done in order to minimize the size of, and thereby effects of, strain energy in the xy plane. Examples of supercells are shown in Fig. 1.

To eliminate the elastic contributions, the corresponding bulk references are calculated with the same distortions in the xy plane. In the z direction the cells are of equilibrium unit length, as are the interface supercells.

All energies have been computed with the spin-polarized GGA-PW91 for the XC energy.¹⁵ As spin-polarized total-energy functionals have local minima, the calculations are started with a fix magnetic moment for the supercell. That moment is taken as the corresponding equilibrium Fe bulk moment. When a calculation starts to converge, the constraint on the polarization is released. Presently, the procedure always results in polarized Fe atoms (weakened at the interface) and unpolarized VN units. Other procedures have not been explored.

The reader is referred to Refs. 25–28 for further details of the DFT method and its plane wave implementation. Here only some specifications are given. A very brief account of the USPP and bulk properties of Fe, V, and VN are given, followed by convergence tests for the interface systems.

A. Ultrasoft pseudopotentials

For Fe and N we use the USPP from Ref. 29, and for V we have generated a USPP similar to that used for Fe.

The potential for V is generated from the $3d^34s^2$ atomic configuration. For the $3d$ angular-momentum channel we use two projector functions and one for the $4s$ channel. Consequently, $4p$ is left for the local potential. The local potential in the USPP scheme may have poor scattering properties. Although a local p channel is used, we find that present USPP shows fairly good scattering properties and chemical

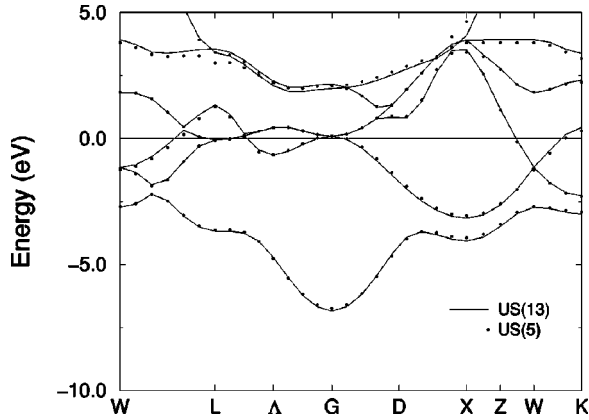


FIG. 2. Band structure for V in the fcc structure for pseudopotentials with and without semi-core shells denoted US(13) and US(5), respectively. The agreement is good except for the higher lying bands. This is probably due to an inferior description of higher p and f states for US(5). The lattice constant is 3.66 Å for both calculations.

hardness. The errors in energy eigenvalues as tested for several different atom configurations are smaller than 11 meV.

To test the USPP for V we have also generated a version including the $3s$ and $3p$ semicore shells. Previous calculations have shown that USPP with semi-core shells are very accurate, as compared to all-electron (AE) methods.^{23,30} With semicore shells, the chemically less active f channel may be used for the local potential. Now, the scattering properties and hardness are found to be excellent. In the following the first version with 5 valence electrons is denoted as US(5) and the second semi-core version as US(13). Figures 2 and 3 show bandstructure states of V and VN bulk calculated with the two USPP's. The agreement is good below the Fermi level, but for higher lying bands the deviations are large. This is probably due to an inferior description of higher p and f states for US(5).

B. Bulk properties of Fe, V, and VN

Table I gives lattice constants a_0 and bulk moduli B for each solid. All calculations are made with a plane-wave cutoff of 340 eV (25 Ry) and the fictitious temperature for

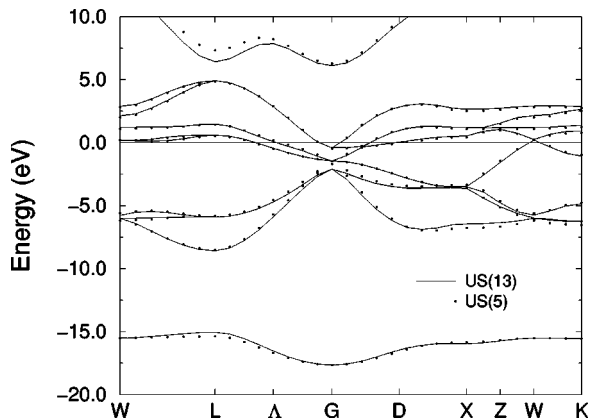


FIG. 3. Same as Fig. 2, but for VN in the nacl structure. The lattice constant is the experimental value 4.14 Å.

TABLE I. Bulk properties of Fe, V, and VN with the present pseudopotentials. The results are compared with all-electron (AE) calculations 23,38 and experimental data 39–41. For Vanadium, results are also given for a pseudopotential with semi-core shells [US(13)].

| | US | AE | Expt. |
|---------------|-------|--------|-------|
| Fe, a_0 (Å) | 2.86 | 2.84 | 2.87 |
| B (GPa) | 152 | 186 | 168 |
| $M(\mu_B)$ | 2.36 | 2.17 | 2.11 |
| | US(5) | US(13) | |
| V, a_0 (Å) | 2.97 | 3.00 | 3.00 |
| B (GPa) | 189 | 176 | 184 |
| VN, a_0 (Å) | 4.09 | 4.13 | 4.14 |
| B (GPa) | 330 | 317 | |

broadening of the electron states is set to 0.1 eV. With these parameters the quantities are well converged.

The comparison with all-electron (AE) methods and experimental data shows that the USPP works very well. Especially the semicore version of V is very close to the all-electron results. The magnetic moment of bcc-Fe is also fairly well reproduced by the USPP.

VN may be viewed as an expanded fcc V metal with N atoms inserted at the interstitial positions. The nonmetal p states form very strong $pd\sigma$ bonds with the $d_{3z^2-r^2, x^2-y^2}$ states on the metal. The partial density of states (DOS) has a pronounced minimum between the bonding and antibonding or nonbonding parts.³¹ There is a strong and quite spherically symmetric charge-density buildup around the N ion, which could be an indication of some ionic character of the VN bond. Nonetheless, VN is a metallic conductor and the partial DOS for p and d states covaries as for a covalent bond.

The above-mentioned contraction of VN and stretch of Fe at equal cost in energy is calculated to be 4.07 Å for the VN nacl lattice constant which equals 2.88 Å for the bcc lattice constant.

C. Convergence tests for interface supercells

As the calculated values of the interface energy are quite small, it is important to test the convergence. For the test calculations a small supercell with $n_{\text{Fe}}=6$ and $n_{\text{VN}}=3$ is used. The supercell has two Fe atoms in each layer and a side of 4.07 Å.

In Fig. 4 the convergence of interface energy w.r.t. PW energy cutoff is shown. It is rapid above 272 eV (20 Ry) and 340 eV (25 Ry), suffices well for the present purposes. The energy integration over the Brillouin zone has been made with a rectangular k -point grid according to the Monkhorst-Pack scheme.³² This sampling is crucial since energies of supercells with different height and hence different Brillouin zones are compared. Previous experience motivates an increased sampling density in the xy plane along with the increase in the z direction.³³ To achieve good convergence the bulk reference grids are matched as well as possible in the reciprocal z direction. A satisfactory convergence of about ± 10 mJ/m² is achieved with a $k_x \times k_y = 10 \times 10$ grid (see Fig. 5).

In fact, non-self-consistent (SC) calculations using the most accurate electron density as input show that the electron

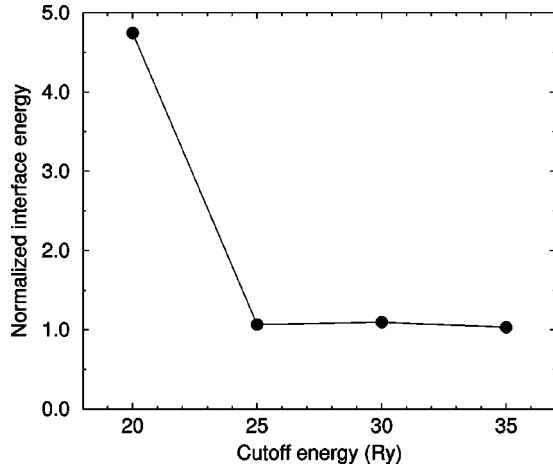


FIG. 4. Convergence with respect to plane-wave cutoff energy of the Fe/VN interface energy for a test supercell. Note that the energy is normalized to the final point.

potential is well converged even for the smallest grid in Fig. 5. In practice this means that unrelaxed and atom-relaxed charge densities may be computed with the smaller grids. Thereafter, the SC densities are used as input to compute total energies with the 10×10 grids for the evaluation of interface energies. The so-called Harris density-functional is used for the non-SC calculations.^{34,35} Several interface energies have been computed SC with the 10×10 grids and the differences compared to the above outlined procedure are negligible.

In order to verify the quality of the US(5) PP, a few interface energies are calculated with the US(13) PP. The test is positive and interface energies differ only with ± 15 mJ/m². Also forces are in fair agreement.

To sum up, the errors due to basis set and use of pseudo-potentials are of the order of ± 30 mJ/m².

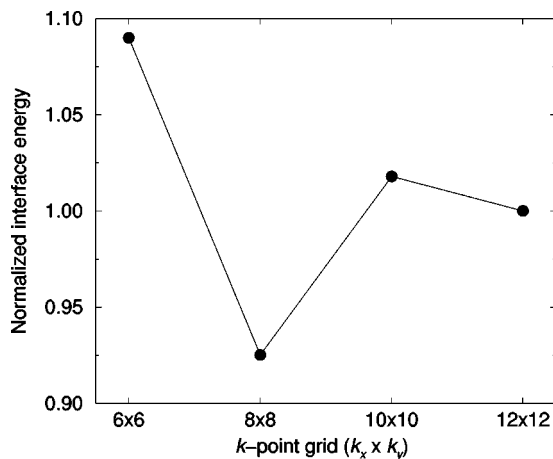


FIG. 5. The figure shows convergence of the Fe/VN interface energy with respect to k -point sampling. The test supercell has $n_{\text{Fe}}=6$ and $n_{\text{VN}}=3$. Each layer has two Fe atoms and a side of 4.07 Å. The results are calculated with a 340 eV PW cutoff and with $k_x \times k_y \times k_z = (6 \times 6 \times 3)$, $(8 \times 8 \times 4)$, $(10 \times 10 \times 4)$, and $(12 \times 12 \times 6)$ grids for the interface cell. The sampling density in the z direction is kept similar to that in the xy plane. Note that the energy is normalized to the final point.

TABLE II. Convergence of interface energy γ with respect to number of Fe layers (n_{Fe}) in the supercell separating two interfaces. The supercells contain two VN layers. The expanded lattice parameter is used for the interface area A in Eq. (2), which gives $A = 4.07^2 = 16.6$ Å. See the text and Eq. (3) for a definition of the change in magnetic moment ΔM . μ_B is the Bohr magneton.

| n_{Fe} | 4 | 8 | 12 |
|-------------------------------|-------|-------|-------|
| γ (mJ/m ²) | 314 | 290 | 294 |
| ΔM (μ_B) | -0.75 | -0.75 | -0.75 |

III. RESULTS FOR FE/VN INTERFACE

A disadvantage of the PW expansion is the necessity of periodic supercells. As an infinite Fe solid is to be simulated, the number of Fe layers must be large enough to avoid interaction between the repeated VN units. In other words, n_{Fe} is increased until electron structure and interface energies stop changing. Table II gives interface energies and change in magnetic moment,

$$\Delta M = M_{\text{Fe/VN}}[n_{\text{Fe}}, n_{\text{VN}}] - M_{\text{Fe}}[n_{\text{Fe}}], \quad (3)$$

for cells with successively increasing Fe thickness. For easier comparisons this change in magnetization is given per Fe interface atom. Evidently, from Table II $n_{\text{Fe}}=8$ is enough. This is also supported by examination of spin-decomposed charge density plots, where no visible difference can be detected between $n_{\text{Fe}}=8$ and $n_{\text{Fe}}=12$ supercells.

A. Unrelaxed interface

The interface properties vary with the thickness of the interface region. Table III presents interface energies [Eq. (2)] for 2, 4, and 6 VN layers. The energy is fairly low even for just two VN layers and decreases further for thicker VN units. The strongest enhancement of charge compared to superposed atomic densities is lobes close to the N ions at the interface. The bonding in VN is dominated by $pd\sigma$ bonds, which is likely to be the case also for the interface and the cause of the strong adherence.

Figure 6 shows charge density and spin polarization averaged in the xy plane for the $n_{\text{VN}}=4$ supercell. Note that the interface charge dipole is contained within the interface and extends less than 2 Å. The first Fe layer shows a depletion in magnetic moment, but the moment heals quickly to bulk value. The spin-decomposed charge densities reveals that V atoms in the first VN layer are very weakly polarized, in the opposite direction compared to Fe, whereas the N atoms remain unpolarized.

TABLE III. Interface energy (γ) of unrelaxed supercells for increasing number of VN layers (n_{VN}). The $n_{\text{VN}}=2$ and 4 interfaces have 8 Fe layers, while the $n_{\text{VN}}=6$ one has 12.

| n_{VN} | 2 | 4 | 6 |
|-------------------------------|-----|-----|-----|
| γ (mJ/m ²) | 290 | 278 | 249 |

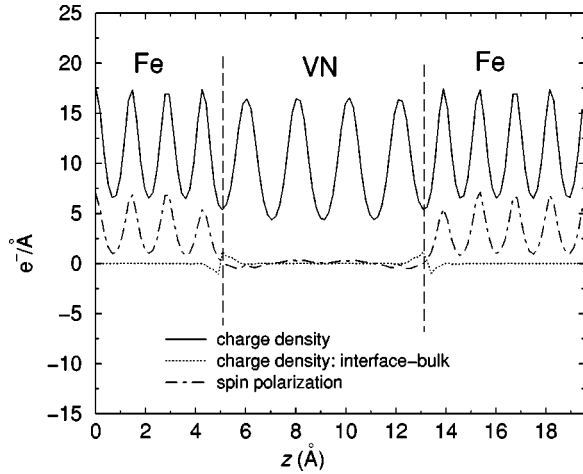


FIG. 6. Charge densities and spin polarization, averaged in the xy plane, for Fe/VN with $n_{\text{VN}}=4$. The charge redistribution creating the interface dipole is confined to less than 4 Å. Also the spin-polarization of Fe heals quickly to its bulk shape.

B. Atom-relaxed interface

The atom relaxations are performed by calculating how the atoms adjust to the Hellman-Feynman forces. The outermost Fe layer(s) are kept fixed, while the rest of the atoms are allowed to relax. A structure is considered completely relaxed when the ionic forces are smaller than $0.10 \text{ eV}/\text{Å}^3$. This corresponds to a residual error in interface energy below 5 mJ/m^2 .

In the unrelaxed solid-on-solid structure the Fe-N distance is quite short and the major effect of the relaxation is an increased Fe-N bondlength. Conversely, the unrelaxed interatomic distances between Fe and V atoms are longer than would be optimal for a hypothetical fcc or bcc bulk. For an even number of VN layers each “pillar” of VN in the z direction moves its N interface atom away from the Fe and its V interface atom towards the Fe. This is exemplified in

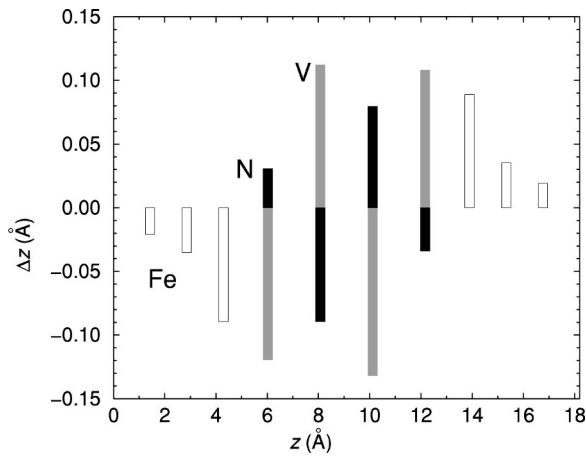


FIG. 7. Atom relaxation for Fe/VN with $n_{\text{VN}}=4$. The z axis represents the atomic positions perpendicular to the interface. The bars are placed at the positions of each atom for the unrelaxed solid-on-solid configuration and show the displacements (Δz) from the unrelaxed positions. Black, shaded, and unfilled bars represents N, V, and Fe atoms, respectively. The major effects are on one hand increased Fe-N bondlength and on the other hand an Fe-V attraction.

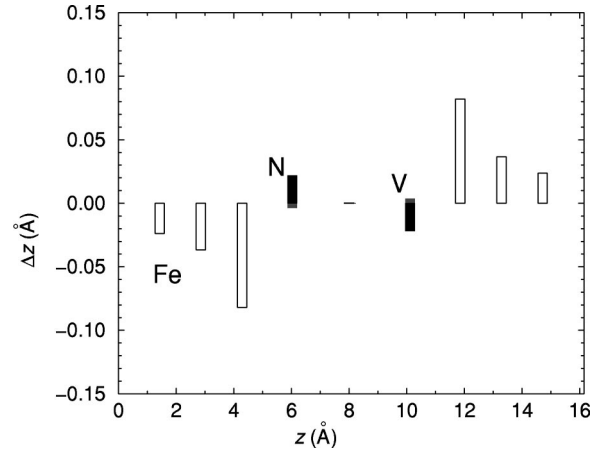


FIG. 8. Same as Fig. 7, but for $n_{\text{VN}}=3$. An almost intact VN bond length is favored and the V interface atoms do not follow the repelled Fe atoms.

Fig. 7 for the $n_{\text{VN}}=4$ structure. For an odd number of VN layers the pillars have the same termination at both interfaces and a motion of pillars cannot take place. Instead, there is only a repelling of the Fe layers (see Fig. 8). The Fe-N bondlength for the relaxed structures is about 1.9 Å, which can be compared to the equilibrium V-N bulk bond of 2.05 Å. The Fe-N bulk bondlength is somewhat shorter (probably about 2.03 Å) than the V-N distance.³¹

The relaxation lowers the interface energies drastically. Table IV gives results for $n_{\text{VN}}=1, 2, 3, 4$, and 6. Already for a single VN layer, forming just half a unit cell, the interface energy is only 245 mJ/m^2 . For two layers it drops to a negative value and seems to converge to about -100 mJ/m^2 . The limited relaxation of V atoms for $n_{\text{VN}}=3$ is not reflected in higher interface energy. This supports the charge density indication that the $pd\sigma$ bond on Fe-N is the most important bond.

The site- and l -projected DOS for the relaxed $n_{\text{VN}}=4$ structure is shown in Fig. 9. The one-electron states are projected onto free-atom orbitals. To avoid too much double-counting the orbitals are truncated at 1.1 Å, since the bondlengths are quite short in VN and at the interfaces.

The third Fe layer [Fe(3) in Fig. 9] has a DOS that is fairly close to that of bulk Fe, where $d_{x^2-y^2, xz, yz}$ and $d_{3z^2-r^2, xy}$ are degenerate. (The not shown fourth layer is very similar to the bulk.) At the interface the Fe(1) d bands are broadened. The $d_{3z^2-r^2}$ and $d_{xz, yz}$ states on Fe(1) have tails down to the bottom of the VN pd band at -8 eV . For the majority spin on Fe(1) and VN(1) there are common peaks at -2 and -4 eV . On the whole, the Fe(1) DOS is rather a mix of the bulk Fe and VN d bands. The magneti-

TABLE IV. Interface energy (γ) for atom relaxed supercells. The $n_{\text{VN}}=2$ and 4 interfaces have 8 Fe layers, while the $n_{\text{VN}}=6$ have 12 and $n_{\text{VN}}=1$ and 3 ones have 7 Fe layers. See the text and Eq. (3) for a definition of the change in magnetic moment ΔM .

| n_{VN} | 1 | 2 | 3 | 4 | 6 |
|-----------------------------------|-------|-------|-------|-------|-------|
| $\gamma \text{ (mJ/m}^2\text{)}$ | 245 | -62 | -83 | -86 | -96 |
| $\Delta M \text{ (}\mu_B\text{)}$ | -0.38 | -0.76 | -0.34 | -0.88 | -0.85 |

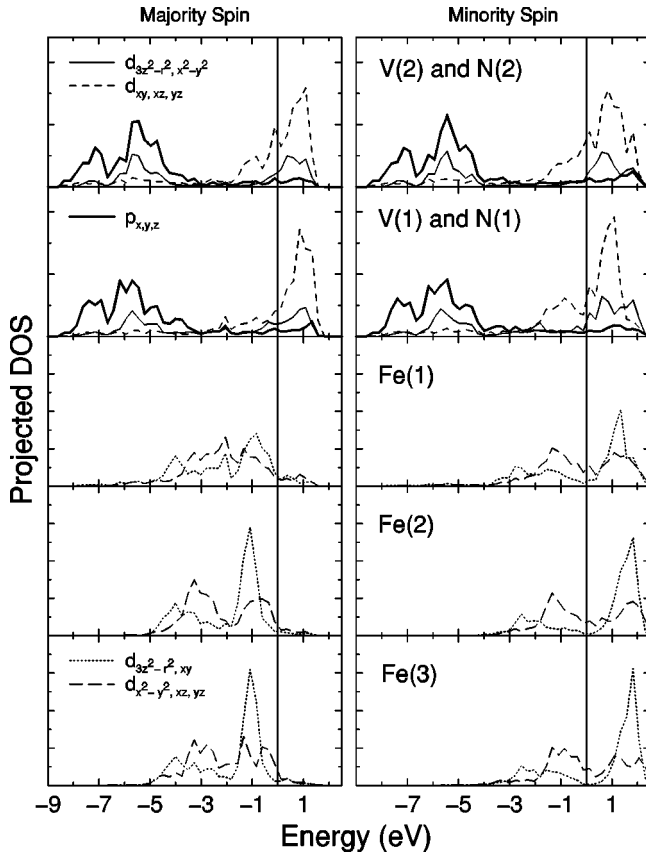


FIG. 9. Projected DOS for Fe/VN with $n_{\text{VN}}=4$. The Fe(1) DOS is rather a mix of the bulk Fe and VN d -bands. The changes in the VN electron structure are much smaller. The $d_{3z^2-r^2}$ on V(1) decreases compared with bulk pd -band due to the loss of one N neighbor at the interface. The DOS retains bulk structure after about three atomic layer for Fe two and for VN. The presented DOS indicates that the bonding across the interface is most likely formed by Fe-N $pd\sigma$ and Fe-V $dd\sigma$ states.

zation of Fe(2) may still be accounted for by mainly a rigid band shift, but for Fe(1) at the interface it is much less of a rigid shift. Table IV gives the change in magnetic moment with an increasing number of VN layers. The reduction is localized to the interface as for the relaxed case in Fig. 6.

The changes in the VN electron structure are much smaller. The $d_{3z^2-r^2}$ on V(1) decreases compared with bulk pd -band due to the loss of one N neighbor at the interface. V(1) also show a weak polarization of the $d_{xy,xz,yz}$ band. According to the presented DOS the bonding across the interface is formed by strong Fe-N $pd\sigma$ and weak Fe-V $dd\sigma$ bonds.

C. N vacancies

Transition-metal nitrides and carbides, both in bulk^{31,26} and precipitated⁶ states are often found to be substoichiometric w.r.t. N and C, which is also likely to be the case for the present model system. As a first step towards a less ideal model interface we have considered N vacancies. For an $n_{\text{VN}}=2$ atom relaxed interface energies are computed for a vacancy concentration of 1/4 and 1/8 with a supercell side of 4.07 \AA and $\sqrt{2} \cdot 4.07 \text{ \AA}$, respectively. For comparison we calculate the interface energy for the $n_{\text{VN}}=4$ structure with

TABLE V. Interface energy (γ) for atom relaxed interfaces with N vacancies. For the $n_{\text{VN}}=2$ interface energies are given for the vacancy concentration 1/4 and also for a twice as large interface with 1/8 concentration. For the concentration of 1/8 the $n_{\text{VN}}=4$ interface energy is also given. That cell has one vacancy in the middle of the slab. See the text and Eq. (3) for a definition of the change in magnetic moment ΔM .

| n_{VN} | 2 (1/4) | 2 (1/8) | 4 (1/8) |
|-------------------------------|---------|---------|---------|
| γ (mJ/m ²) | 136 | 110 | 114 |
| ΔM (μ_B) | -0.72 | -0.63 | -0.78 |

1/8 vacancy concentration. Here, the vacant site is located in the middle of the VN unit. Results for interface energies are given in Table V.

The VN bulk references are also computed with the same vacancy structure as the interface VN units in order to comply with the purposes outlined for Eq. (2). The difference between interface energies in Table IV and V should not be interpreted as a formation energy for the vacancies. The increase in the calculated interface energies constitutes an additional cost to create a precipitate with vacancies. To theoretically determine if vacancies are energetically favorable or not requires the computation of (free) energies for the interface system with an N atom at some other preferred position in the Fe matrix. The present results should be regarded as an indication of changes in electronic structure and interface energy due to vacancies.

The interface energies increase considerably and varies rather little for the different position and number of vacancies. The increase is equivalent to about 0.1 eV/vacancy or 0.01-0.03 eV/V atom. This energy cost is rather high, but should be compensated by a reduction of elastic energy since the VN lattice constant becomes smaller with vacancies (not considered in this study). Another possibility could be vacancy ordering, which may lower vacancy formation energies in transition metal carbides and nitrides also at low temperatures.³⁶

Figure 10 compares site-projected DOS for bulk and interface structures with and without vacancies. As reported earlier, vacancies create states in the anti- and nonbonding region of the pd band.²³ The presence of the interface produces a similar effect. Moreover, the interface Fe atoms tends to show less fcc and more bcc structure for the substoichiometric interface.

IV. DISCUSSION AND CONCLUSIONS

The theory for bonding in transition-metal nitrides and carbides outlined by the group around Grimvall³¹ will be exploited to interpret the calculated electron structure and interface energies.

The experimental variation with average number of valence electrons for the enthalpy of formation has a rather sharp maximum around TiC, ZrC, and HfC and an almost flat region for compounds with increasing number of valence electrons.³¹ In the picture of Grimvall and coworkers the minimum in the total DOS of VN (see Fig. 10) separates bonding states from anti- and nonbonding regions. The filling of the pd band is shown to dominate the trends in en-

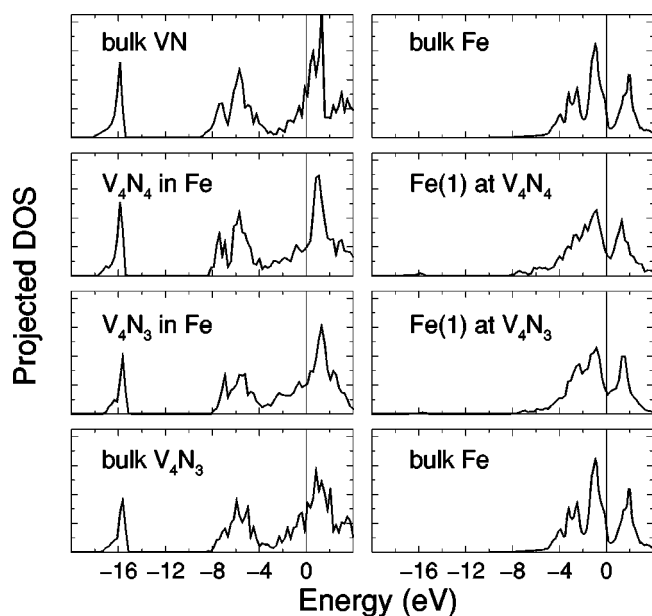


FIG. 10. Projected DOS for Fe/VN with $n_{\text{VN}}=2$, with and without an N vacancy. The DOS for the interface layers for VN and Fe are compared with the corresponding one for bulk VN and Fe. The left panels show bulk (bottom and top) and interface (middle) DOS for VN units with and without a vacancy. The middle right panels show the DOS for an Fe atom at the interfaces. The DOS is taken for the Fe atom at intact interface [i.e., the Fe(1) atom is not adjacent to the vacant N(2) site]. For comparison the top and bottom left panels show the Fe bulk DOS. The $x=3/4$ N vacancy in bulk VN creates states in the DOS minimum region. The change in DOS for the interfaces is similar to the change with the vacancy.

thalpy over other contributions, such as changes in volume and crystal structure for a range of compounds. Accordingly, the optimal number of valence electrons is six per metal-carbon/nitride pair (TiC, ZrC, and HfC). Compounds with 1-2 “excess” electrons are believed to first fill antibonding states causing the enthalpy of formation to fall sharply, while additional electrons mainly fill nonbonding states and consequently the decrease in enthalpy of formation is much less pronounced.

Compounds with an excess of electrons tends to have vacancies and/or form more complex crystal structures.^{31,36} VN has two excess electrons filling the band above the minimum and the removal of N atoms destroys bonding and antibonding $pd\sigma$ states. Some of the loss in bonding energy is compensated for by moving antibonding electrons to nonbonding metal-metal states.³⁶ Hence, the DOS peaks in bulk VN with N vacancies (Fig. 10) can be interpreted as precursors of the fcc metal DOS.³⁶

The introduction of an Fe interface provides a possibility to form $pd\sigma$ bonds between Fe and N atoms. Consequently, the interface N atoms have an environment similar to that in bulk VN, and the interface Fe atoms can form stronger bonds than in bulk Fe. In contrast, the interface V atoms lose some of their $pd\sigma$ bonds. In this picture the presence of the interface is much like the effects of N vacancies. To compensate for the lost N neighbors the V atoms may transfer electrons to states across the interface and to non-bonding states within VN itself. Since VN is in the flat region of the enthalpy of

formation curve it seems reasonable that the interface energy may become very low.

Now, if N atoms are removed from VN, the atoms around the vacancy will try to compensate for the lost bonds by filling nonbonding states. With vacancies *inside* the VN unit the strong Fe-N bonds remain. At the interface some or all of the nonbonding states on the V atoms are already occupied. As a result, they can at least not fully contribute to the described compensation. Thus, the interface energy increases. With vacancies *at the interface* strong Fe-N bonds are lost. Since the iron atoms have more valence electrons than V they should be less able to compensate the loss than V in VN bulk. However, because of the presumably good metallic bonding between V-Fe, the absolute increase in interface energy may still be fairly small.

Inspection of the difference in charge densities with and without vacancies supports the above picture. The thinner cells show an enhancement of charge along V-Fe nearest neighbors at the interface side with the vacant site. For the thicker VN units there is a small charge build-up between V neighbors below the vacancy. Vanadium atoms above the vacancy (at the interface) do not show such a build-up.

Following the above band-filling arguments VN is less sensitive to changes in average number of valence electrons than TiC. Accordingly the Fe/TiC interface energy should be considerably higher than the Fe/VN one. The interface energies of the intermediate Fe/TiN and Fe/VC systems may be inbetween or perhaps even lower. However, if Fe/VN has the smallest interface energy of these three systems substitutional elements with fewer (more) valence electrons would increase (decrease) the interface energy for Fe/VN. It would be interesting to explore these arguments by calculating interface energies, where V and N are successively substituted by other transition metals and carbon, respectively.

In general, semicoherent interface energies are expected to be around 200–300 mJ/m², which also is assumed in the mentioned modeling.⁸ In comparison, the present atom-relaxed energies are small. The stoichiometric structures have even negative interface energies. This might seem worrisome, but there are also elastic contributions to the total interface energy which are *not* included here. The cost in (elastic) energy to compress an eight atom VN unit cell with 0.05 Å is about 70 meV (35 mJ/m²) per VN layer, which is of the same order as the chemical interface energy.

Furthermore, the strain of the bulk references only costs energy, but could provide extra space for the interface relaxation. This may result in artificially lowered interface energies. However, the differences in volume are small compared with the relaxations and this matter has not been further investigated.

V. SUMMARY

Steels represent by far the most widely-used metallic materials, easy to manufacture and to specify, and with an extensive range of mechanical properties. Strengthening of iron and its alloys is usually achieved by the combined use of several mechanisms. Non-shearable precipitates may be obtained with carbide and nitride formers.^{4,5} The formation of small precipitates within grains has its virtues in design of creep-resistant steels. The particles is believed to substan-

tially hinder the motion of dislocations and thus increase the creep strength. Knowing the properties of such precipitates is of key importance for the understanding of nucleation, growth, and effects on dislocations. The Fe/VN system serves here as an important model for such situations.

In this paper a first-principles calculational method,^{25–28} based on density-functional theory, plane waves and pseudo-potentials, is successfully applied to a calculation of atomic structure, electron structure, and interface energy of the relaxed Fe/VN interface. Values for the interface energy have been calculated for VN units of varying thickness. Relaxations of atom positions are found to lower energies considerable on a relative scale. Already a single layer VN has a low-interface energy of 245 mJ/m², while two, three, four, and six layers of VN are shown to have even smaller, and negative, values. Nitrogen vacancies are also considered and their presence raises the interface energies. For the present model system, it is today prohibitively costly to calculate any optimal vacancy concentration or distribution of vacancies. The experimentally observed precipitates have a concentration of vacancies around 10–15 %.⁶ Accordingly, the interface energies with the 1/8 concentration should be the most appropriate ones. In conclusion, the chemical interface energy for a 2–4 layer thin VN unit with N vacancies is calculated to be around 100 mJ/m². Modelling and experiments suggest nucleation of precipitates as thin as 2–4 layers of VN.^{6,8} The present calculations are consistent with such sizes.

The smallness of the interface energy is an important result and the fact that this smallness can be related to features of the electron structure. The electron structure is interpreted in terms of a simple bonding theory established earlier for bulk transition-metal carbides.^{31,23} In short, the bonding

across the interface appear mainly in the VN DOS minima and is of $pd\sigma$ and $dd\sigma$ character, which form nacl and fcc nearest-neighbors bonds between Fe-N and Fe-V, respectively. For both VN and Fe the electron structure heals to bulk in about 3–4 atomic layers.

This study urges on more extensive and systematic studies of interfaces between Fe and transition-metal carbides and nitrides, in order to establish more firm relations between electron-structural features and mesoscopic quantities like the interface energy. Together with other timely studies, it show the great potential of first-principles total-energy methods for calculating materials parameters and for increased understanding of materials properties.

ACKNOWLEDGMENTS

I would like to thank Professor H.-O. Andrén for introducing me to the Fe/VN interface problem and also for valuable discussions together with Professor J. Ågren (Department of Materials Science, Royal Institute of Technology) and Professor G. Grimvall (Department of Theoretical Physics, Royal Institute of Technology). It is also a pleasure to thank Professor B. Lundqvist for discussions and proofreading the manuscript. This work has been supported financially by the Swedish Foundation for Strategic Research (SSF) via Materials Consortium No. 9 and by allocation of computer time at Chalmers (UNICC) and the Swedish Center for Parallel Computers (PDC). The DFT calculations have been performed with a computer code developed in the group of Professor J. Nørskov, Technical University of Denmark.³⁷ The code has been ported to and further optimized for the UNICC computers by L. Bengtsson. I also wish to acknowledge D. Vanderbilt for providing us with the pseudopotential generator program.

¹A. Kelly, *Strong Solids*, 2nd ed. (Oxford University Press, Oxford, 1973).

²G. B. Olson, *Science* **277**, 1237 (1997).

³A. P. Sutton and R. W. Balluffi, *Interfaces in Crystalline Materials* (Oxford University Press, Oxford, 1996).

⁴W. C. Leslie and E. Hornbogen in *Physical Metallurgy*, (North-Holland, Amsterdam, 1996), edited by R. W. Cahn and P. Haasen Vol. 2.

⁵R. W. K. Honeycombe and H. K. D. H. Bhadeshia, *STEELS Microstructure and Properties* (Arnold, London, 1995).

⁶L. Lundin, S. Fällman, and H.-O. Andrén, *Mater. Sci. Technol.* **13**, 233 (1997).

⁷M. Hättestrand, M. Schwind and H.-O. Andrén, *Mater. Sci. Eng. A*. (to be published).

⁸Å. Gustafson and J. Ågren, *J. Acta Mater.* **46**, 81 (1998).

⁹W. Blum, in *Materials Science and Technology*, edited by R. W. Cahn, P. Haasen, and E. J. Kramer (VCH, Berlin, 1992), Vol. 6.

¹⁰B. Sundman, B. Janson, and J. O. Andersson, *CALPHAD: Comput. Coupling Phase Diagrams Thermochem.* **9**, 153 (1985).

¹¹P. Hohenberg and W. Kohn, *Phys. Rev.* **136**, B864 (1964).

¹²W. Kohn and L. Sham, *Phys. Rev.* **140**, A1133 (1965).

¹³R. Jones and O. Gunnarsson, *Rev. Mod. Phys.* **61**, 689 (1989).

¹⁴K. Laasonen, A. Pasquarello, R. Car, Changyol Lee, and D. Vanderbilt, *Phys. Rev. B* **47**, 10 142 (1993).

¹⁵J. P. Perdew, J. A. Chevary, S. H. Vosko, K. A. Jackson, M. A. Pederson, D. J. Singh, and C. Fiolhais, *Phys. Rev. B* **46**, 6671 (1992).

¹⁶M. Körling and J. Häglund, *Phys. Rev. B* **45**, 13 293 (1992).

¹⁷J. Häglund, *Phys. Rev. B* **47**, 566 (1993).

¹⁸J. E. James, J. R. Smith, G.-L. Zhao, and D. J. Srolovitz, *Phys. Rev. Lett.* **53**, 13 883 (1996).

¹⁹R. Wu, A. J. Freeman, and G. B. Olson, *Phys. Rev. B* **53**, 7504 (1996).

²⁰Sheng N. Sun, N. Kioussis, and M. Ciftan, *Phys. Rev. B* **54**, 3074 (1996).

²¹M. W. Finnis, *J. Phys.: Condens. Matter* **8**, 5811 (1996).

²²Jun-Hyung Cho and M. Scheffler, *Phys. Rev. B* **53**, 10 685 (1996).

²³E. G. Moroni, G. Kresse, J. Hafner, and J. Fürthmüller, *Phys. Rev. B* **56**, 15 629 (1997).

²⁴S. G. Louie, S. Froyen, and M. L. Cohen, *Phys. Rev. B* **26**, 1738 (1982).

²⁵M. T. Yin and M. L. Cohen, *Phys. Rev. B* **25**, 7403 (1982).

²⁶M. C. Payne, M. P. Teter, D. C. Allen, T. A. Arias, and J. D. Joannopoulos, *Rev. Mod. Phys.* **64**, 1045 (1992).

²⁷B. Hammer, K. W. Jacobsen, V. Milman, and M. C. Payne, *J. Phys.: Condens. Matter* **4**, 10 453 (1992).

²⁸G. Kresse and J. Fürthmüller, *Phys. Rev. B* **54**, 11 169 (1996).

- ²⁹L. B. Hansen (unpublished).
- ³⁰K. Stokbro, Phys. Rev. B **53**, 6869 (1996).
- ³¹J. Häglund, A. F. Guillermet, G. Grimvall, and M. Körling, Phys. Rev. B **48**, 11 685 (1993).
- ³²H. J. Monkhorst and J. D. Pack, Phys. Rev. B **13**, 5188 (1976).
- ³³J. Hartford, B. von Sydow, G. Wahnström, and B. I. Lundqvist, Phys. Rev. B **58**, 2487 (1998).
- ³⁴J. Harris, Phys. Rev. B **31**, 1770 (1985).
- ³⁵W. M. C. Foulkes and R. Haydock, Phys. Rev. B **39**, 12 520 (1989).
- ³⁶V. Ozoliņš and J. Häglund, Phys. Rev. B **48**, 5069 (1993).
- ³⁷DACAPO version 1.30 [Center for Atomic Scale Materials Physics (CAMP), Denmark Technical University, Denmark, 1997].
- ³⁸V. Ozoliņš and M. Körling, Phys. Rev. B **48**, 18 304 (1993).
- ³⁹C. Kittel, *Introduction to Solid State Physics* (Wiley, New York, 1976).
- ⁴⁰A. F. Guillermet and G. Grimvall, Phys. Rev. B **40**, 10 582 (1989).
- ⁴¹Compiled by P. Eckerlin and H. Kandler, *Numerical Data and Functional Relationships in Science and Technology*, edited by K.-H. Hellwege, Landolt-Börnstein, New Series, Group III, Vol. 6, Pt. I (Springer-Verlag, Berlin, 1971).